Stabilizing Ion and Radical Ion Pair States in a Paramagnetic Endohedral Metallofullerene/π-Extended Tetrathiafulvalene Conjugate

Yuta Takano,[†] Shota Obuchi,[†] Naomi Mizorogi,[†] Raúl García,[‡] M. Ángeles Herranz,[‡] Marc Rudolf,[§] Silke Wolfrum,[§] Dirk M. Guldi,*,[§] Nazario Martín,*,[‡,||] Shigeru Nagase,*,[⊥] and Takeshi Akasaka*,[†]

[†]Life Science Center of Tsukuba Advanced Research Alliance, University of Tsukuba, Tsukuba, Ibaraki 305-8577, Japan

[‡]Departamento de Química Orgánica I, Facultad de Química, Universidad Complutense, E-28040 Madrid, Spain

[§]Department of Chemistry and Pharmacy Interdisciplinary Center for Molecular Materials (ICMM), Friedrich-Alexander-Universität Erlangen-Nürnberg, Egerlandstrasse 3, 91058 Erlangen, Germany

[||]IMDEA−Nanoscience, Campus de Cantoblanco, E-28049 Madrid, Spain

[⊥]Fukui Institute for Fundamental Chemistry, Kyoto University, Kyoto 606-8103, Japan

S *Supporting Information*

ABSTRACT: Electron donor−acceptor conjugates of paramagnetic endohedral metallofullerenes and π-extended tetrathiafulvalene (exTTF) were synthesized, characterized, and probed with respect to intramolecular electron transfer involving paramagnetic fullerenes. UV−vis−NIR absorption spectroscopy complemented by electrochemical measurements attested to weak electronic interactions between the electron donor, exTTF, and the electron acceptor, La@C$_{82}$, in the ground state. In the excited state, photoexcitation powers a fast intramolecular electron transfer to yield an ion and radical ion pair state consisting of one-electron-reduced La@C$_{82}$ and of one-electron-oxidized exTTF.

Endohedral metallofullerenes (EMFs)[1] are known for their rich electronic properties and as such bear great potential in fields ranging from chemistry[2] and physics[3] to bioscience[4] and nanoscience.[5] Among fullerenes in general, paramagnetic EMFs have garnered much attention because of their unique electronic and magnetic properties, which are quite different from those of the closely related nonparamagnetic endofullerenes. However, their rather low production efficiency has hampered the advancement of elucidating and clarifying the intrinsic properties of paramagnetic EMFs.

La@C$_{82}$ has been extensively investigated as a prototype paramagnetic fullerene, since it was demonstrated that a family of lanthanum-containing fullerenes could be produced and that extraction with toluene yielded mostly La@C$_{82}$.[6] La@C$_{82}$ has an electronic structure that is best described as [La]$^{3+}$[C$_{82}$]$^{3−}$ with an open-shell electronic character that is a consequence of the transfer of three electrons from La to C$_{82}$.[7] In La@C$_{82}$, the resulting electron spin imposes a unique chemical reactivity comparable to that of a radical character.[8] The latter is believed to induce magnetism on the molecular scale[9] and/or enhance electronic conductivity.[1,3b]

We recently reported on reversible *inter*molecular electron transfer reactions in solution using paramagnetic La@C$_{82}$ in combination with organic electron donors.[9] Such electron transfer systems feature remarkable thermochromic and solvatochromic characteristics and bear great potential as novel hybrid materials for optoelectronic and magnetic applications. To date, however, reports regarding *intra*molecular electron transfer in paramagnetic EMFs are unprecedented. In this regard, an important goal of the present work was to prove that an open-shell electronic structure like that of La@C$_{82}$ is stabilized upon photoinduced reduction, thus enhancing the interest of paramagnetic EMFs in devices such as photovoltaic cells, in which the lifetime of the charge-separated state is a key issue.

In the current work, we synthesized a unique electron donor−acceptor conjugate consisting of an electron donor linked to the electron-accepting La@C$_{82}$. We selected the π-extended tetrathiafulvalene, 9,10-bis(1,3-dithiol-2-ylidene)-9,10-dihydroanthracene (exTTF), as the electron donor, since its electron transfer reactions with fullerenes have been studied both in the ground and excited states in various electron donor−acceptor conjugates.[10]

La@C$_{82}$−exTTF (**1**) was synthesized by a 1,3-dipolar cycloaddition reaction of an azomethine ylide generated in situ from *n*-octylglycine and 2-formyl-9,10-bis(1,3-dithiol-2-ylidene)-9,10-dihydroanthracene (exTTF-CHO)[11] to La@C$_{82}$ [Scheme 1 and Figure S1 in the Supporting Information

Scheme 1. Synthesis of La@C$_{82}$−exTTF
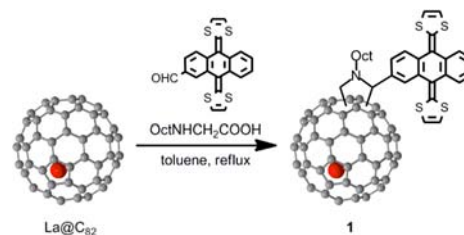
(SI)].[2a,12,13] After a one-step HPLC separation, a single fraction containing two products was obtained (Figures S2 and S3). Hereinafter, this fraction is denoted as "**1a&1b**" to indicate the presence of **1a** and **1b** as a mixture.

Further support for this notion was provided by electron spin resonance (ESR) and NMR spectroscopy. The observed ESR spectrum of **1a&1b** revealed a broad asymmetric octet signal (Figure 1), indicating that **1a** and **1b** have open-shell electronic
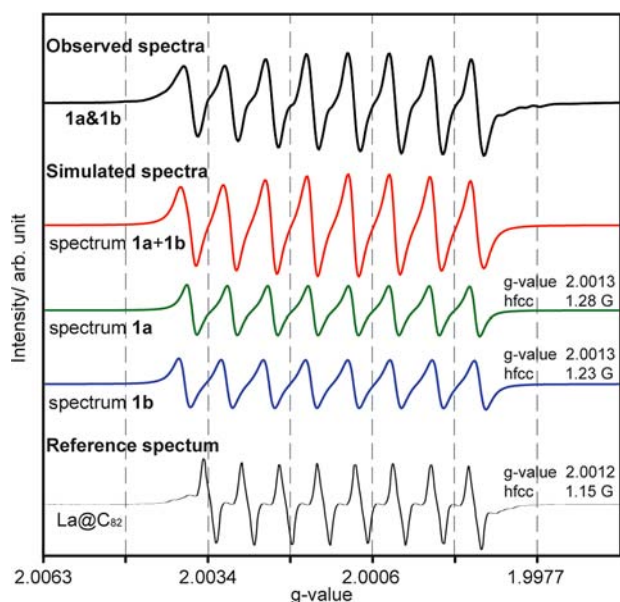

Figure 1. Observed ESR spectrum of **1a&1b** in degassed toluene, two simulated octet signals (spectrum **1a** and spectrum **1b**), their combination in a 1:1 ratio (spectrum **1a+1b**), and the reference spectrum of pristine La@C$_{82}$.

structures in line with that of pristine La@C$_{82}$, and this spectrum was well-fitted by a combined spectrum (spectrum **1a** +**1b**) consisting of two simulated octet signals (spectrum **1a** and spectrum **1b**) in 1:1 ratio. In addition, the NMR signals of the ESR-silent anionic forms of **1a** and **1b**, as obtained by bulk electrolysis, revealed two half-intensity singlet signals at 4.65 and 4.57 ppm. These were assigned to methyne protons (Figures S4 and S5). From a comparison of these half-intensity signals with those from the methylene protons at 6.12 and 5.92 ppm, we conclude the existence of two isomers, that is, metallofulleropyrrolidines **1a** and **1b**. In summary, our NMR and ESR assays suggested that **1a&1b** is approximately a 1:1 mixture of **1a** and **1b**.

Regarding the molecular structures of **1a** and **1b**, density functional theory (DFT) calculations provide sound insight into the addition site of the CH$_2$N(Oct)CH−exTTF moiety. From the DFT-optimized structure of La@C$_{82}$,[14] we infer that the lowest unoccupied molecular orbital (LUMO) is localized on the C−C bond in which the two carbons show the highest π-orbital axis vector (POAV) values[15] and the most positive charge densities. Notably, only the C21−C23 bond fulfills these criteria (Table 1). The electron-accepting LUMO plays a dominating role in the addition reaction of azomethine ylides.[16] With this in mind, C21−C23 was identified as the most feasible candidate for the addition site to form **1**.

Because of the asymmetric nature of azomethine ylides, cycloadditions at C21−C23 may generate diastereomers of four types. The DFT-optimized structures of the four possible

Table 1. The Four Highest Mulliken Charge Densities and POAV Values in La@C$_{82}$^{a,b}

Carbon number	Charge density	POAV value
C14	0.000	10.90
C18	0.004	10.85
C21	0.002	10.41
C23	0.006	10.62

^{a}Values were calculated at the M06-2X/3-21G[H,C,N,S],LANL2DZ-[La] level of theory. ^{b}The values for all of the carbon atoms are shown in Table S1 in the SI.

isomers are portrayed in Figure S6. In fact, the results from the ^{1}H NMR experiments indicated that **1a** and **1b** have equivalent methylene protons and inequivalent methyne protons, strongly suggesting that both isomers feature methylene hydrogens linked to the carbon adjacent to the addition position (i.e., either C21 or C23). The two most stable DFT-optimized structures, which likely correspond to **1a** and **1b**, possess methylene hydrogens linked to the carbon adjacent to C23 (Figure 2). In addition, the overall selectivity relates to the fact
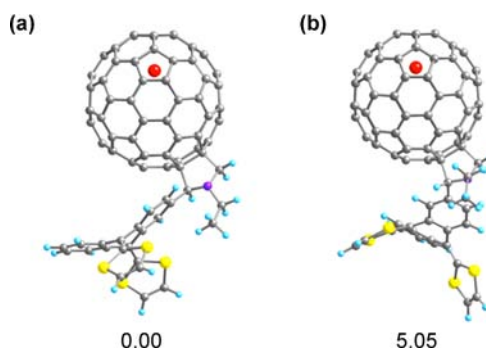

Figure 2. Optimized structures and relative energies (in kcal/mol) of the two feasible isomers of **1** (in which the octyl groups have been substituted with ethyl groups for simplification) calculated at the M06-2X/6-31G(d)[H,C,N,S],LANL2DZ[La] level of theory. The structures are [5,6]-isomers in which exTTF is situated (a) in front of the page and (b) behind the page. The structures in (a) and (b) are likely to correspond to **1a** and **1b**.

that C23 is the carbon that carries most of the positive charge and is thus susceptible to attack by the negatively charged part of the asymmetric azomethine ylide in the cycloaddition reaction.

The ground-state electronic properties of **1a** and **1b** were probed by means of absorption spectroscopy complemented by cyclic voltammetry (CV) and differential pulse voltammetry (DPV). The absorption spectra of **1a&1b** demonstrated that La@C$_{82}$−exTTF retains the electronic properties of La@C$_{82}$ (Figure S7) and exTTF (Figure S8). In particular, the characteristic absorption of exTTF at 429 nm remained mostly unperturbed in the spectrum of **1a&1b**.

On the basis of the CV measurements, we identified the redox-active sites in **1a&1b**. The oxidative part (+0.05 V) is dominated by the oxidation of exTTF,[17] although the first oxidation (−0.04 V) is La@C$_{82}$-centered.[2a] This hypothesis was further supported by theoretical calculations, which indicated that the singly occupied MO is localized on La@C$_{82}$ in the

most stable optimized structure of La@C$_{82}$−exTTF (Figure S9). All of the reductions correlated with those of La@C$_{82}$ (−0.38, −1.32, and −1.66 V)[2a] (Figure S10 and Table S2). Importantly, all of the oxidations and reductions were observed as clear peaks, indicating that the two metallofulleropyrrolidines **1a** and **1b** have comparable redox properties. These characteristics are in excellent agreement with the results of ESR and absorption measurements. In fact, we consider that the similarity of the electronic properties of **1a** and **1b** provided sufficient grounds to study **1a&1b** with respect to the intrinsic electron transfer properties of La@C$_{82}$−exTTF.

To evaluate the excited-state interactions as a complement to the above-described ground-state interactions, we investigated La@C$_{82}$−exTTF in relation to La@C$_{82}$−Ph and exTTF-CHO as references by means of femtosecond pump−probe experiments following 387 nm excitation. Excitation of exTTF-CHO at 387 nm generated a fairly short lived exTTF-centered excited state (Figure S11). The spectral characteristics of the latter excited state were transient maxima around 455, 615, and 915 nm as well as transient bleaching at a wavelength below 450 nm. Because of strong second-order spin couplings, exTTF-centered excited states tend to decay rapidly, that is, within a time window of up to ∼10 ps. From a monoexponential fit of the decay at, for example, the 615 nm maximum, we derived a rate constant of $(1.2 \pm 0.2) \times 10^{12}$ s^{-1}.

For the La@C$_{82}$ reference, La@C$_{82}$−Ph, in which a phenyl group replaces exTTF, maxima at 455, 550, 695, 900, and 1140 nm and a minimum at 950 emerged as a consequence of the formation of the La@C$_{82}$ doublet excited state (Figure S12). The latter maxima were subject to monoexponential decay in the form of a rapid intersystem crossing with a lifetime of 20 ± 3 ps (corresponding to a rate constant of 5.0×10^{10} s^{-1}), yielding the energetically lower-lying quartet excited state. For the La@C$_{82}$-centered quartet excited state, we noted a several nanosecond-lived transient spectrum with maxima at 450, 560, 705, 910, and 1140 nm.

In the case of La@C$_{82}$−exTTF, considering the absorption features of both constituents under 387 nm excitation, we must assume the excitation of both the La@C$_{82}$ and exTTF constituents. Indeed, in transient absorption measurements with La@C$_{82}$−exTTF with excitation at 387 nm in either tetrahydrofuran (THF) (Figure 3) or cyclohexylisonitrile (Figure S13), we noted the instantaneous formation of exTTF- and La@C$_{82}$-centered excited states all throughout the visible and near-IR regions, respectively. Most notable were the maxima at 465 and 645 nm, attesting to the successful excitation of exTTF. The latter peaks bear a great resemblance to the 455 and 615 nm maxima seen in the experiments with exTTF-CHO (Figure S14). Within less than 10 ps, the exTTF excited state transforms into one-electron-oxidized exTTF. Evidence for the oxidative electron transfer was provided by the 670 nm maximum and the ground-state bleaching around 430 nm. We ascribe this change in oscillator strength to the oxidation of exTTF, since both features are characteristic markers seen upon one-electron oxidation of exTTF by pulse radiolysis (Figure S15).[18] The additional feature at 460 nm relates to the one-electron-reduced La@C$_{82}$. In terms of the La@C$_{82}$-centered doublet excited state, the maxima at 455, 550, 895, and 1160 nm as well as the minimum at 950 nm were in perfect agreement with the transient features seen for La@C$_{82}$−Ph that lacks exTTF, thus corroborating the successful excitation of La@C$_{82}$. Within ∼10 ps, the La@C$_{82}$ doublet excited state characteristics decay. Representative time
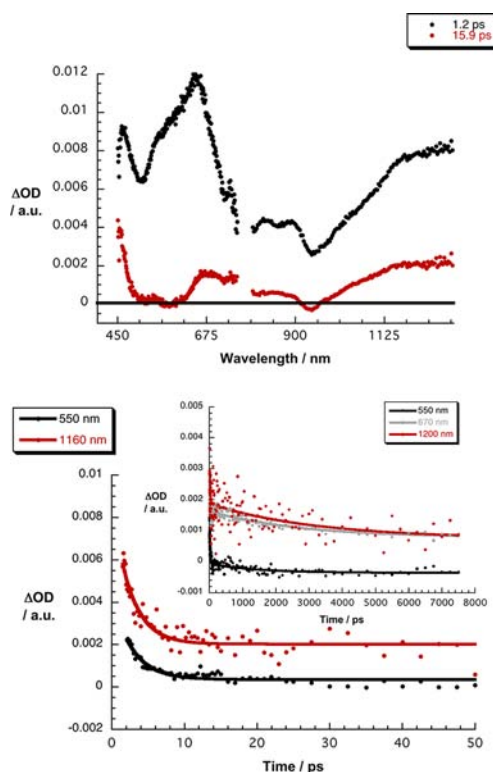

Figure 3. (top) Differential absorption spectra (visible and near-IR) obtained upon femtosecond pump−probe experiments (387 nm) of La@C$_{82}$−exTTF (10^{-5} M) in argon-saturated THF with time delays of 1.2 ps (black spectrum) and 15.9 ps (red spectrum) at room temperature. (bottom) Time-absorption profiles at 550 nm (black) and 1160 nm (red) monitoring the charge separation. Monoexponential fits are shown. Inset: time−absorption profiles of the spectra shown above at 550 nm (black), 670 nm (gray), and 1220 nm (red) monitoring the charge separation and charge recombination. Biexponential fits are shown.

absorption profiles at the 550 and 1160 nm maxima are displayed in Figure 3. A closer look at the absorption characteristics sheds light onto the nature of the photoproduct. Of particular importance is the observation that the spectroscopic pattern with maxima at 860 and 1220 nm as well as a minimum at 945 nm is a good match to the one that developed during the electrochemical one-electron reduction of La@C$_{82}$−Ph, which had maxima at 925/1275 nm and a minimum at 1050 nm (Figure S16). We ascribe the underlying shifts, which are particularly pronounced for the 1050 nm minimum, to electronic interactions between La@C$_{82}$ and exTTF. Thus, we reach the important conclusion that the two excited states, exTTF at 2.7 eV and La@C$_{82}$ at 0.88 eV,[19] power an intramolecular electron transfer to yield an energetically low-lying La@C$_{82}$$^{\bullet-}$−exTTF$^{\bullet+}$ radical ion pair state (0.43 eV) (Figure S17).

From multiwavelength analyses, we derived the charge separation and charge recombination dynamics (Figure 3 and Figure S14). In line with the different excited state energies (see above), the La@C$_{82}$$^{\bullet-}$−exTTF$^{\bullet+}$ radical ion pair state evolves from the exTTF-centered and La@C$_{82}$-centered excited states with lifetimes (rate constants) of 4.3 ± 0.5 ps (2.3×10^{11} s^{-1}) and 6.3 ± 0.5 ps (1.5×10^{11} s^{-1}), respectively. The charge recombination, which reinstates the ground state, is remarkably slow: a global analysis gave values of 2.4 ± 0.5 ns (4.1×10^{8}

s^{-1}) in THF and 1.1 ± 0.3 ns (9.1×10^8 s^{-1}) in cyclohexylisonitrile.

In short, we have designed, synthesized, and probed a novel electron donor−acceptor conjugate consisting for the first time of a paramagnetic $La@C_{82}$ and an electron-donating exTTF. Notably, $La@C_{82}$−exTTF was obtained as a mixture of two regioisomeric metallofulleropyrrolidines, **1a** and **1b**. The **1a&1b** mixture was characterized by spectroscopic and electrochemical methods, which confirmed that **1a** and **1b** possess quasi-equivalent electronic properties. While the ground states of **1a** and **1b** lack appreciable electronic interactions between $La@C_{82}$ and exTTF, the electronically excited state undergoes electron transfer deactivation of the photoexcited $La@C_{82}$. Quite remarkable is the fact that the unique properties of $La@C_{82}$, an open-shell electronic structure that undergoes stabilization upon reduction, assists in stabilizing the radical ion pair state for more than 2 ns.

■ ASSOCIATED CONTENT

ⓈSupporting Information

Synthetic procedures and structural characterization of compounds, spectral data for **1**, and Cartesian coordinates of the optimized structures of **1**. This material is available free of charge via the Internet at http://pubs.acs.org.

■ AUTHOR INFORMATION

Corresponding Author

guldi@chemie.uni-erlangen.de; nazmar@quim.ucm.es; nagase@ims.ac.jp; akasaka@tara.tsukuba.ac.jp

Notes

The authors declare no competing financial interest.

■ ACKNOWLEDGMENTS

■ REFERENCES

(1) For recent reviews, see: (a) *Chemistry of Nanocarbons*, Akasaka, T., Wudl, F., Nagase., S., Eds.; Wiley: Chichester, U.K., 2010. (b) Rudolf, M.; Wolfrum, S.; Guldi, D. M.; Feng, L.; Tsuchiya, T.; Akasaka, T.; Echegoyen, L. *Chem.—Eur. J.* **2012**, *18*, 5136.

(2) (a) Chaur, M. N.; Melin, F.; Ortiz, A. L.; Echegoyen, L. *Angew. Chem., Int. Ed.* **2009**, *48*, 7514. (b) Lu, X.; Akasaka, T.; Nagase, S. *Chem. Commun.* **2011**, *47*, 5942.

(3) (a) Ross, R. B.; Cardona, C. M.; Guldi, D. M.; Sankaranarayanan, S. G.; Reese, M. O.; Kopidakis, N.; Peet, J.; Walker, B.; Bazan, G. C.; Van Keuren, E.; Holloway, B. C.; Drees, M. *Nat. Mater.* **2009**, *8*, 208.

(b) Sato, S.; Seki, S.; Honsho, Y.; Wang, L.; Nikawa, H.; Luo, G.-F.; Lu, J.; Haranaka, M.; Tsuchiya, T.; Nagase, S.; Akasaka, T. *J. Am. Chem. Soc.* **2011**, *133*, 2766.

(4) (a) Shultz, M. D.; Wilson, J. D.; Fuller, C. E.; Zhang, J.; Dorn, H. C.; Fatouros, P. P. *Radiology* **2011**, *261*, 136. (b) Fillmore, H. L.; Shultz, M. D.; Henderson, S. C.; Cooper, P.; Broaddus, W. C.; Chen, Z. J.; Shu, C.-Y.; Zhang, J.; Ge, J.; Dorn, H. C.; Corwin, F.; Hirsch, J. I.; Wilson, J.; Fatouros, P. P. *Nanomedicine* **2011**, *6*, 449.

(5) Dorn, H. C.; Fatouros, P. P. *Nanosci. Nanotechnol. Lett.* **2010**, *2*, 65.

(6) Chai, Y.; Guo, T.; Jin, C.; Haufler, R. E.; Chibante, L. P. F.; Fure, J.; Wang, L.; Alford, J. M.; Smalley, R. E. *J. Phys. Chem.* **1991**, *95*, 7564.

(7) (a) Nagase, S.; Kobayashi, K. *Chem. Phys. Lett.* **1993**, *214*, 57. (b) Nagase, S.; Kobayashi, K. *Chem. Phys. Lett.* **1994**, *228*, 106. (c) Nagase, S.; Kobayashi, K. *J. Chem. Soc., Chem. Commun.* **1994**, 1837.

(8) Takano, Y.; Yomogida, A.; Nikawa, H.; Yamada, M.; Wakahara, T.; Tsuchiya, T.; Ishitsuka, M. O.; Maeda, Y.; Akasaka, T.; Kato, T.; Slanina, Z.; Mizorogi, N.; Nagase, S. *J. Am. Chem. Soc.* **2008**, *130*, 16224.

(9) Tsuchiya, T.; Sato, K.; Kurihara, H.; Wakahara, T.; Maeda, Y.; Akasaka, T.; Ohkubo, K.; Fukuzumi, S.; Kato, T.; Nagase, S. *J. Am. Chem. Soc.* **2006**, *128*, 14418.

(10) (a) Martín, N.; Sánchez, L.; Herranz, M. A.; Illescas, B.; Guldi, D. M. *Acc. Chem. Res.* **2007**, *40*, 1015. (b) Brunetti, F. G.; López, J. L.; Atienza, C.; Martín, N. *J. Mater. Chem.* **2012**, *22*, 4188.

(11) Takano, Y.; Herranz, M. A.; Martín, N.; Radhakrishnan, S. G.; Guldi, D. M.; Tsuchiya, T.; Nagase, S.; Akasaka, T. *J. Am. Chem. Soc.* **2010**, *132*, 8048.

(12) Maggini, M.; Scorrano, G.; Prato, M. *J. Am. Chem. Soc.* **1993**, *115*, 9798.

(13) For Prato reactions, see: (a) Cai, T.; Ge, Z.; Iezzi, E. B.; Glass, T. E.; Harich, K.; Gibson, H. W.; Dorn, H. C. *Chem. Commun.* **2005**, 3594. (b) Cardona, C.; Kitaygorodskiy, M. A.; Ortiz, A.; Herranz, M. A.; Echegoyen, L. *J. Org. Chem.* **2005**, *70*, 5092.

(14) Frisch, M. J.; Trucks, G. W.; Schlegel, H. B.; Scuseria, G. E.; Robb, M. A.; Cheeseman, J. R.; Scalmani, G.; Barone, V.; Mennucci, B.; Petersson, G. A.; Nakatsuji, H.; Caricato, M.; Li, X.; Hratchian, H. P.; Izmaylov, A. F.; Bloino, J.; Zheng, G.; Sonnenberg, J. L.; Hada, M.; Ehara, M.; Toyota, K.; Fukuda, R.; Hasegawa, J.; Ishida, M.; Nakajima, T.; Honda, Y.; Kitao, O.; Nakai, H.; Vreven, T.; Montgomery, J. A., Jr.; Peralta, J. E.; Ogliaro, F.; Bearpark, M.; Heyd, J. J.; Brothers, E.; Kudin, K. N.; Staroverov, V. N.; Kobayashi, R.; Normand, J.; Raghavachari, K.; Rendell, A.; Burant, J. C.; Iyengar, S. S.; Tomasi, J.; Cossi, M.; Rega, N.; Millam, J. M.; Klene, M.; Knox, J. E.; Cross, J. B.; Bakken, V.; Adamo, C.; Jaramillo, J.; Gomperts, R.; Stratmann, R. E.; Yazyev, O.; Austin, A. J.; Cammi, R.; Pomelli, C. J.; Ochterski, W.; Martin, R. L.; Morokuma, K.; Zakrzewski, V. G.; Voth, G. A.; Salvador, P.; Dannenberg, J. J.; Dapprich, S.; Daniels, A. D.; Farkas, O.; Foresman, J. B.; Ortiz, J. V.; Cioslowski, J. Fox, D. J. *Gaussian 09*, revision A.02; Gaussian, Inc.: Wallingford, CT, 2009.

(15) Haddon, R. C. *Science* **1993**, *261*, 1545.

(16) Sawai, K.; Takano, Y.; Izquierdo, M.; Filippone, S.; Martín, N.; Slanina, Z.; Mizorogi, N.; Waelchli, M.; Tsuchiya, T.; Akasaka, T.; Nagase, S. *J. Am. Chem. Soc.* **2011**, *133*, 17746.

(17) Herranz, M. A.; Yu, L.; Martín, N.; Echegoyen, L. *J. Org. Chem.* **2003**, *68*, 8379.

(18) (a) Guldi, D. M.; Sánchez, L.; Martín, N. *J. Phys. Chem. B* **2001**, *105*, 7139. (b) Jones, A. E.; Christensen, C. A.; Perepichka, D. F.; Batsanov, A. S.; Beeby, A.; Low, P. J.; Bryce, M. R.; Parker, A. W. *Chem.—Eur. J.* **2001**, *7*, 973.

(19) Fujitsuka, M.; Ito, O.; Kobayashi, K.; Nagase, S.; Yamamoto, K.; Kato, T.; Wakahara, T.; Akasaka, T. *Chem. Lett.* **2000**, 902.

16106

dx.doi.org/10.1021/ja3055386 | *J. Am. Chem. Soc.* 2012, 134, 16103−16106